Eidgenössische Technische Hochschule Zürich

Ecole polytechnique fédérale de Zurich
Politecnico federale di Zurigo
Swiss Federal Institute of Technology Zurich

Robust finite volume schemes for simulating waves in the solar atmosphere

S. Mishra

Research Report No. 2010-37
October 2010

Seminar für Angewandte Mathematik
Eidgenössische Technische Hochschule
CH-8092 Zürich
Switzerland

ROBUST FINITE VOLUME SCHEMES FOR SIMULATING WAVES IN THE SOLAR ATMOSPHERE

S. MISHRA

Abstract. We present well-balanced high-resolution finite volume schemes for simulating waves in the outer solar atmosphere. The schemes approximate the stratified MHD equations with an upwind discretization of the Godunov-Powell source term and a locally hydrostatic pressure reconstruction that preserves discrete steady states. The paper summarizes recent articles [4, 5, 6].

1. Introduction

The study of the sun is of paramount importance. In particular, the solar climate is a key determinant of climate on earth. Solar weather impacts us directly in the form of magnetic storms that affect the electrical grid and indirectly through solar flares and prominences that pose a hazard for satellites and space vehicles. The sun (see figure 1) consists of the following parts: an inner core where most of the solar energy is generated, a radiative zone, a convective zone and the *outer* solar atmosphere. In turn, the solar atmosphere consists of the photosphere (the visible part of the sun), the chromosphere and the corona. It is well known that there is a considerable variation in the temperature of the outer solar atmosphere. The temperature of the photosphere is around 6000 K and the chromosphere is almost isothermal at about 10000 K. However, the temperature in the corona is about 10^6 K (see figure 1). This massive variation in temperature takes place in a very narrow layer (as compared to the typical solar length scale) termed as the *transition region*.

Many interesting questions about the solar atmosphere remain unanswered. Examples include how the solar energy is transferred to the overlaying chromospheric and coronal plasmas and heats them. The above issues are related to the role played by waves and oscillations in the solar atmosphere. It is well known ([1]) that waves carry energy from the base of the solar atmosphere (in the convection zone) upto the chromosphere and the corona. While traveling up the atmosphere, these waves interact with the magnetic field of the sun. This complex interaction between waves and the magnetic field is a possible candidate for explaining the intricate dynamics of the solar atmosphere [1].

1.1. Models of the outer solar atmosphere.

Matter in the sun exists in the form of *plasma* i.e., magnetized fluid. The outer solar atmosphere can be modeled by the equations of *stratified*

The results reported here are obtained jointly with F. G. Fuchs, A. D. McMurry, N. H. Risebro (University of Oslo, Norway) and K . Waagan (University of Maryland, College park, U. S. A).

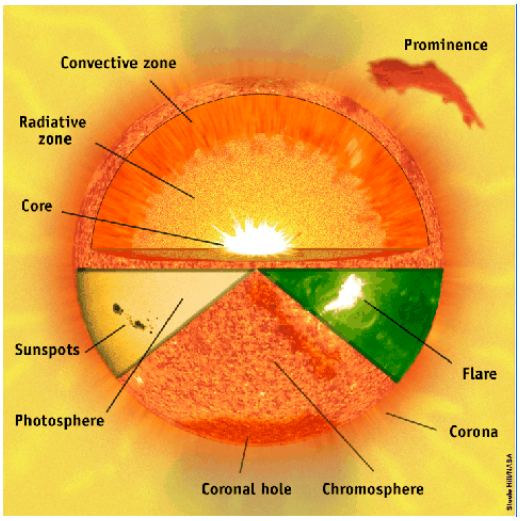

(a) Parts of the sun

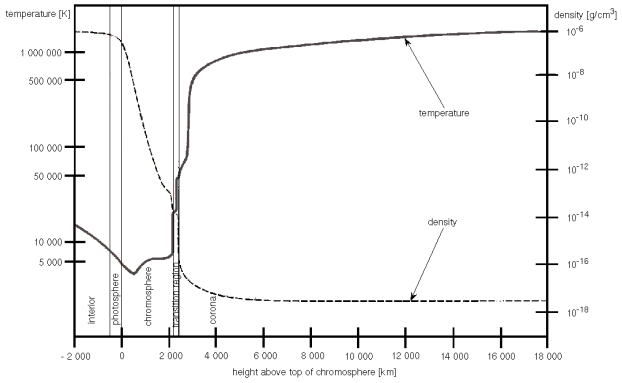

(b) Temperature distribution

Magnetohydrodynamics (sMHD):

$$
\begin{aligned}
\rho_t + \operatorname{div}(\rho \mathbf{u}) &= 0, \\
(\rho \mathbf{u})_t + \operatorname{div}\left(\rho \mathbf{u} \otimes \mathbf{u} + \left(p + \frac{1}{2}\left|\overline{\mathbf{B}}\right|^2\right) I - \overline{\mathbf{B}} \otimes \overline{\mathbf{B}}\right) &= -\rho g \mathbf{e}_3, \\
\overline{\mathbf{B}}_t + \operatorname{div}\left(\mathbf{u} \otimes \overline{\mathbf{B}} - \overline{\mathbf{B}} \otimes \mathbf{u}\right) &= 0 \\
E_t + \operatorname{div}\left(\left(E + p + \frac{1}{2}\left|\overline{\mathbf{B}}\right|^2\right)\mathbf{u} - \left(\mathbf{u} \cdot \overline{\mathbf{B}}\right)\overline{\mathbf{B}}\right) &= -\rho g \left(\mathbf{u} \cdot \mathbf{e}_3\right), \\
\operatorname{div}(\overline{\mathbf{B}}) &= 0,
\end{aligned}
\tag{1.1}
$$

where ρ is the density, $\mathbf{u} = \{u_1, u_2, u_3\}$ and $\overline{\mathbf{B}} = \{\overline{B}_1, \overline{B}_2, \overline{B}_3\}$ are the velocity and magnetic fields respectively, p is the thermal pressure, g is the constant acceleration due to gravity , $\mathbf{e}_3$ represents the unit vector in the vertical (z-) direction. E is the total energy, for simplicity determined by the ideal gas equation of state:

$$
E = \frac{p}{\gamma - 1} + \frac{1}{2}\rho \left|\mathbf{u}\right|^2 + \frac{1}{2}\left|\overline{\mathbf{B}}\right|^2, \tag{1.2}
$$

where $\gamma > 1$ is the adiabatic gas constant. The above equations need to be augmented with suitable initial and boundary conditions.

Our primary objective is to simulate waves in the solar atmosphere. We will present robust and highly efficient numerical schemes to simulate waves in the outer solar atmosphere in this paper. We summarize some recent results ([4],[5],[6]) in this direction.

2. The ideal MHD equations

The first step in designing efficient schemes for the stratified MHD equations is to discretize the ideal MHD equations obtained from (1.1) by setting the gravity $g = 0$. The resulting

equations are a system of conservation laws of the form,

$$\mathbf{U}_t + \mathbf{F}_x + \mathbf{G}_y + \mathbf{H}_z = 0. \tag{2.1}$$

Here $\mathbf{U} = \{\rho, \mathbf{u}, \overline{\mathbf{B}}, E\}$ and the fluxes $\mathbf{F}, \mathbf{G}, \mathbf{H}$ can be read from (1.1). The MHD equations are hyperbolic but not strictly hyperbolic. Furthermore, the shock structure of MHD equations is quite complicated on account of the non-strict hyperbolicity and the non-convexity of these equations.

The absence of explicit solution formulas or theoretical results implies that numerical simulations are the main tools for studying MHD and related equations. Finite volume methods ([9]) are among the most popular frameworks for approximating conservation laws like (2.1). We consider (2.1) in $\mathbf{x} = (x, y, z) \in [X_l, X_r] \times [Y_l, Y_r] \times [Z_b, Z_t]$ and discretize it by a uniform grid in all directions with the grid spacing $\Delta x, \Delta y$ and Δz. We set $x_i = X_l + i\Delta x$, $y_j = Y_l + j\Delta y$ and $z_k = Z_b + k\Delta z$. The indices are $0 \le i \le N_x$, $0 \le j \le N_y$ and $0 \le k \le N_z$. Set $x_{i+1/2} = x_i + \Delta x/2$, $y_{j+1/2} = y_j + \Delta y/2$ and $z_{k+1/2} = z_k + \Delta z/2$, and let $\mathcal{C}_{i,j,k} = [x_{i-1/2}, x_{i+1/2}) \times [y_{j-1/2}, y_{j+1/2}) \times [z_{k-1/2}, z_{k+1/2})$ denote a typical cell. The cell average of the unknown state vector $\mathbf{W}$ (approximating $\mathbf{U}$) over $\mathcal{C}_{i,j,k}$ at time t^n is denoted $\mathbf{W}^n_{i,j,k}$. By integrating the conservation law over the cell $\mathcal{C}_{i,j,k}$ and the time interval $[t^n, t^{n+1})$ with $t^{n+1} = t^n + \Delta t^n$, where the time-step Δt^n is determined by a suitable CFL condition results in a standard (first-order in space and time) finite volume scheme written down as

$$\begin{aligned}\mathbf{W}^{n+1}_{i,j,k} = \mathbf{W}^n_{i,j,k} - \Delta t^n \left(\frac{\mathbf{F}^n_{i+1/2,j,k} - \mathbf{F}^n_{i-1/2,j,k}}{\Delta x} + \frac{\mathbf{G}^n_{i,j+1/2,k} - \mathbf{G}^n_{i,j-1/2,k}}{\Delta y} \right) \\ - \frac{\Delta t^n}{\Delta z} (\mathbf{H}^n_{i,j,k+1/2} - \mathbf{H}^n_{i,j,k-1/2}).\end{aligned} \tag{2.2}$$

The numerical fluxes $\mathbf{F}$, $\mathbf{G}$ and $\mathbf{H}$ are determined in terms of (approximate) Riemann solvers. A wide variety of approximate Riemann solvers are available for the MHD system; see [8, 3] and references therein.

A crucial issue that arises in approximating the MHD equations is a discretization of the divergence constraint in (1.1). The standard finite volume scheme (2.2) *will not* preserve a discrete version of the constraint, leading to numerical instabilities and oscillations, see [11]. Recipes for treating the divergence constraint include the projection method [2] and methods based on staggering [11] (and references therein).

An alternative involves adding the Godunov-Powell source term to the MHD equations resulting in the balance law,

$$\begin{aligned}\mathbf{U}_t + \mathbf{F}_x + \mathbf{G}_y + \mathbf{H}_z = \mathbf{s}. \\ \mathbf{s} = \{-\overline{\mathbf{B}}(\mathrm{div}\overline{\mathbf{B}}), -\mathbf{u}(\mathrm{div}\overline{\mathbf{B}}), -(\mathbf{u}\cdot\overline{\mathbf{B}})(\mathrm{div}\overline{\mathbf{B}})\}.\end{aligned} \tag{2.3}$$

The above equations are (formally) equivalent to the standard form of MHD equations (1.1) without gravity. The added advantages of the Godunov-Powell form (2.3) are its Galilean invariance and symmetrizability. Furthermore, the magnetic field in (2.3) satisfies the divergence transport equation:

$$(\mathrm{div}\overline{\mathbf{B}})_t + \mathrm{div}(\mathbf{u}(\mathrm{div}\overline{\mathbf{B}})) = 0. \tag{2.4}$$

Hence, initial divergence errors are transported out of the domain enabling us to treat the divergence constraint approximately in a stable manner. The method was proposed in [10] but recent papers ([3]) show that the additional source terms in (2.3) need to discretized in a suitable manner for numerical stability.

2.1. **HLL three wave solvers and upwind discretizations of the Godunov-Powell source terms.** Following [4], we present a judicious combination of an approximate Riemann solver and upwind source discretization for the Godunov-Powell MHD system. For simplicity, we consider (2.3) in one space dimension and write the resulting system as,

$$\mathbf{U}_t + \mathbf{F}_x = \mathbf{s^1}. \tag{2.5}$$

Here, the source $\mathbf{s^1} = \mathbf{s^1}(\mathbf{U}, (\overline{B}_1)_x)$ involves a non-conservative product and needs to be discretized carefully. The corresponding first-order finite volume scheme for (2.3) is

$$\mathbf{W}_i^{n+1} = \mathbf{W}_i^n - \frac{\Delta t^n}{\Delta x}(\mathbf{F}_{i+1/2}^n - \mathbf{F}_{i-1/2}^n) + \Delta t^n \mathbf{S}_i^{1,n}. \tag{2.6}$$

We will approximate the eight waves in the MHD Riemann problem with three waves, i.e, two representing the outermost fast waves and a middle wave approximating the material contact discontinuity. The approximate solution and fluxes are given by

$$\mathbf{W}^{H_3} = \begin{cases} \mathbf{W}_L & \text{if } \frac{x}{t} \leq s_L, \\ \mathbf{W}_L^* & \text{if } s_L < \frac{x}{t} < s_M, \\ \mathbf{W}_R^* & \text{if } s_M < \frac{x}{t} < s_R, \\ \mathbf{W}_R & \text{if } s_R \leq \frac{x}{t}, \end{cases} \qquad \mathbf{F}^{H_3} = \begin{cases} \mathbf{F}_L & \text{if } \frac{x}{t} \leq s_L, \\ \mathbf{F}_L^* & \text{if } s_L < \frac{x}{t} < s_M, \\ \mathbf{F}_R^* & \text{if } s_M < \frac{x}{t} < s_R, \\ \mathbf{F}_R & \text{if } s_R \leq \frac{x}{t}. \end{cases} \tag{2.7}$$

We set $\pi_1 = p + \frac{\overline{B}_2^2 + \overline{B}_3^2}{2}$. The outer wave speeds s_L and s_R model the fast magneto-sonic waves and are defined as in [8]. In order to describe the solver, we need to determine the speed of the middle wave s_M and the intermediate states $\mathbf{W}_L^*, \mathbf{W}_R^*$. The middle wave models a material contact discontinuity. Hence, the velocity field and the tangential magnetic fields are assumed to be constant across the middle wave. This allows us to define $\mathbf{u}^* = \mathbf{u}_L^* = \mathbf{u}_R^*$, $\overline{B}_2^* = \overline{B}_{2L}^* = \overline{B}_{2R}^*$ and $\overline{B}_3^* = \overline{B}_{3L}^* = \overline{B}_{3R}^*$. The normal magnetic field $\overline{B}_1$ is not assumed to be constant but jumps only across the middle wave (modeling the linear degenerate "divergence wave" implied by (2.4)), and $\overline{B}_1$ is constant across the outer waves. The intermediate states are determined by local conservation across the two outermost waves and the middle wave resulting in,

$$s_\sigma \mathbf{W}_\sigma^* - \mathbf{F}_\sigma^* = s_\sigma \mathbf{W}_\sigma - \mathbf{F}_\sigma, \quad s_M \mathbf{W}_R^* - s_M \mathbf{W}_L^* = \mathbf{F}_R^* - \mathbf{F}_L^* + \mathbf{s}^{1,*} \tag{2.8}$$

where $\sigma \in \{L, R\}$ and

$$\mathbf{s}^{1,*} = \begin{pmatrix} 0 \\ -\frac{\overline{B}_{1R}^2 - \overline{B}_{1L}^2}{2}) \\ -\left(\overline{B}_2^*\right)\left(\overline{B}_{1R} - \overline{B}_{1L}\right) \\ -\left(\overline{B}_3^*\right)\left(\overline{B}_{1R} - \overline{B}_{1L}\right) \\ -\mathbf{u}^*\left(\overline{B}_{1R} - \overline{B}_{1L}\right) \\ -u_1^* \frac{\overline{B}_{1R}^2 - \overline{B}_{1L}^2}{2} - \left(u_2^* \overline{B}_2^* + u_3^* \overline{B}_3^*\right)\left(\overline{B}_{1R} - \overline{B}_{1L}\right) \end{pmatrix}. \tag{2.9}$$

This amounts to integrating the source $\mathbf{s}^1$ across the wave fan.

Applying the conservation relations, we obtain (check [5], section 3.1.2 for details) the following intermediate states,

$$\begin{aligned}
\rho_\theta^* &= \rho_\theta \frac{u_{1\theta} - s_\theta}{s_M - s_\theta}, \quad \pi_{1\theta}^* = \pi_{1\theta} + \rho_\theta (u_{1\theta} - s_\theta)(u_{1\theta} - s_M), \quad \theta \in \{L, R\}, \\
s_M = u_1^* &= \frac{\pi_{1R} - \pi_{1L} + \rho_R u_{1R}(u_{1R} - s_R) - \rho_L u_{1L}(u_{1L} - s_L)}{\rho_R (u_{1R} - s_R) - \rho_L (u_{1L} - s_L)}, \\
u_\sigma^* &= \frac{\zeta c_\sigma - \xi d_\sigma}{\alpha\zeta + \xi^2}, \quad \overline{B}_\sigma^* = \frac{-\alpha d_\sigma - \xi c_\sigma}{\alpha\zeta + \xi^2}, \quad \sigma \in \{2, 3\} \\
E_\theta^* &= \frac{1}{s_M - s_\theta} \Big(E_\theta \left(u_{1\theta} - s_\theta\right) + \pi_{1\theta} u_{1\theta} - \pi_{1\theta}^* s_M + \frac{\overline{B}_{1\theta}^2}{2} \left(u_{1\theta} - s_M\right) \\
&\quad + \left(\overline{B}_{1\theta}\right) \left(\overline{B}_{2\theta} u_{2\theta} + \overline{B}_{3\theta} u_{3\theta} - \overline{B}_{2\theta}^* u_{2\theta}^* - \overline{B}_{3\theta}^* u_{3\theta}^* \right) \Big), \quad \theta \in \{L, R\}, \\
c_\sigma &= \rho_R u_{\sigma R} \left(u_{1R} - s_R\right) - \rho_L u_{\sigma L} \left(u_{1L} - s_L\right) - \left(\overline{B}_{1R} \overline{B}_{\sigma R} - \overline{B}_{1L} \overline{B}_{\sigma L} \right), \\
d_\sigma &= \overline{B}_{\sigma R} \left(u_{1R} - s_R\right) - \overline{B}_{\sigma L} \left(u_{1L} - s_L\right) - \left(\overline{B}_{1L} u_{\sigma L} - \overline{B}_{1R} u_{\sigma R} \right), \\
\alpha &= \rho_R \left(u_{1R} - s_R\right) - \rho_L \left(u_{1L} - s_L\right), \quad \zeta = s_R - s_L, \quad \xi = \overline{B}_{1R} - \overline{B}_{1L}.
\end{aligned}$$

.

The intermediate fluxes are obtained in terms of the intermediate states by local conservation (2.8),

$$\mathbf{F}_L^* = \mathbf{F}_L + s_L(\mathbf{W}_L^* - \mathbf{W}_L), \quad \mathbf{F}_R^* = \mathbf{F}_R + s_R(\mathbf{W}_R^* - \mathbf{W}_R).$$

The discrete source term takes the form,

$$\mathbf{S}_i^{1,n} = \mathbf{s}_{i-1/2}^{1,*} \chi_{(s_{M,i-1/2} \geq 0)} + \mathbf{s}_{i+1/2}^{1,*} \chi_{(s_{M,i+1/2} < 0)}, \tag{2.10}$$

where $\mathbf{s}_{i\pm1/2}^{1,*}$ is defined in analogy to (2.9).

For the three dimensional form of the equations, the fluxes $\mathbf{G}, \mathbf{H}$ and the sources $\mathbf{S}^2$ and $\mathbf{S}^3$ can be defined analogously to obtain the following finite volume scheme:

$$\begin{aligned}
\mathbf{W}_{i,j,k}^{n+1} &= \mathbf{W}_{i,j,k}^n - \Delta t^n \left(\frac{\mathbf{F}_{i+1/2,j,k}^n - \mathbf{F}_{i-1/2,j,k}^n}{\Delta x} + \frac{\mathbf{G}_{i,j+1/2,k}^n - \mathbf{G}_{i,j-1/2,k}^n}{\Delta y} \right) \\
&\quad - \Delta t^n \left(\frac{\mathbf{H}_{i,j,k+1/2}^n - \mathbf{H}_{i,j,k-1/2}^n}{\Delta z} - \mathbf{S}_{i,j,k}^{1,n} - \mathbf{S}_{i,j,k}^{2,n} - \mathbf{S}_{i,j,k}^{3,n} \right),
\end{aligned} \tag{2.11}$$

for the three dimensional version of the MHD equations with Godunov-Powell source term (2.3).

The above scheme (2.11) is first-order accurate in both space and time. Second-order of accuracy in space is obtained by using non-oscillatory piecewise linear reconstructions using minmod, ENO and WENO limiters. Second-order accuracy in time is obtained using strong stability preserving Runge-Kutta methods. Details of how these procedures are adapted for the MHD equations are described in [4].

2.2. **Code.** The above schemes are implemented in the form a publicly available code called *ALSVID* [7]. The implementation involves a modular C++ based code with Python scripts at both the front and back ends. The plotting routines in one and two dimensions use *Matplotlib* and in three dimensions, we use *Mayavi 2* for the graphics. The code is parallelized using scaled MPI and can handle very large number of parallel cores. ALSVID is adapted to perform solar simulations and the resulting code is termed *SURYA*.

2.3. **Numerical experiment: Orszag-Tang Vortex.** This well-known test case (see [11] for details of the initial data and computational domain) is computed with the second-order version of the scheme and the computed pressure on two different mesh sizes, i.e, 200×200 and 4000×4000 mesh points is shown in figure 1. The figure shows that the shocks as well as the vortices are resolved very well. In particular, the 4000×4000 plot shows the impressive stability of the scheme on ultra fine meshes.

2.4. **Numerical experiment: Cloud-Shock interaction.** The interaction of a fast shock with a high density bubble (see [11] for details) is computed with a second-order version of the scheme and the total energy and magnetic pressure are shown in figure 2.

2.5. **Numerical experiment: isothermal blast wave.** This standard test case easily exhibits spurious behavior if the equations are not properly discretized. The equation of state is isothermal in this case, i.e, $p = \rho$, the computational domain is $[0,1] \times [0,1]$ and the initial data are

$$\{\mathbf{u}, B_1, B_{2,3}\}_{t=0} = \{\mathbf{0}, \frac{5}{\sqrt{\pi}}, 0\}, \quad \rho_0 = \begin{cases} 100 & \text{if } |(x,y)-(0.5,0.5)| \leq (0.05), \\ 0. & \text{otherwise} \end{cases}$$

In order to illustrate the necessity of the *upwinded* Godunov-Powell source term, we also considered the central source discretisation of [10] and schemes with the Godunov-Powell source set to zero. The results with three schemes: no source, central source and upwind source (2.11), with a second-order discretization, are presented in figure 3. They clearly illustrate the necessity of using the Godunov-Powell source term as well as discretizing it in the correct manner.

3. Schemes for Stratified MHD.

We model the outer solar atmosphere in terms of the following modified *stratified MHD equations*:

$$\begin{aligned}
&\rho_t + \mathrm{div}(\rho \mathbf{u}) = 0, \\
&(\rho\mathbf{u})_t + \mathrm{div}\left(\rho\mathbf{u}\otimes\mathbf{u} + \left(p + \frac{1}{2}|\mathbf{B}|^2 + \widetilde{\mathbf{B}}\cdot\mathbf{B}\right) I - \mathbf{B}\otimes\mathbf{B} - \widetilde{\mathbf{B}}\otimes\mathbf{B} - \mathbf{B}\otimes\widetilde{\mathbf{B}}\right) \\
&\qquad\qquad = -\left(\mathbf{B}+\widetilde{\mathbf{B}}\right)(\mathrm{div}\mathbf{B}) - \rho g \mathbf{e}_3, \\
&\mathbf{B}_t + \mathrm{div}\left(\mathbf{u}\otimes\mathbf{B} - \mathbf{B}\otimes\mathbf{u} + \mathbf{u}\otimes\widetilde{\mathbf{B}} - \widetilde{\mathbf{B}}\otimes\mathbf{u}\right) = -\mathbf{u}(\mathrm{div}\mathbf{B}), \\
&E_t + \mathrm{div}\left(\left(E + p + \frac{1}{2}|\mathbf{B}|^2 + \mathbf{B}\cdot\widetilde{\mathbf{B}}\right)\mathbf{u} - (\mathbf{u}\cdot\mathbf{B})\mathbf{B} - \left(\mathbf{u}\cdot\widetilde{\mathbf{B}}\right)\mathbf{B}\right) \\
&\qquad\qquad = -(\mathbf{u}\cdot\mathbf{B})(\mathrm{div}\mathbf{B}) - \rho g\left(\mathbf{u}\cdot\mathbf{e}_3\right),
\end{aligned} \tag{3.1}$$

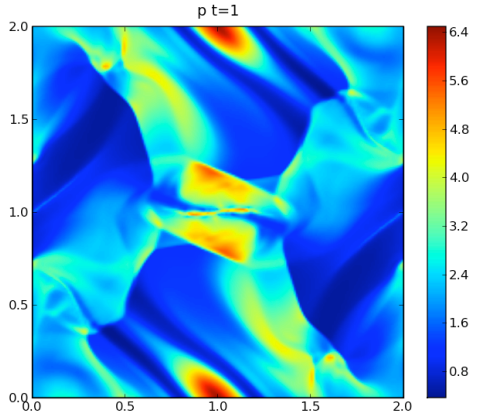

(c) 200^2 mesh

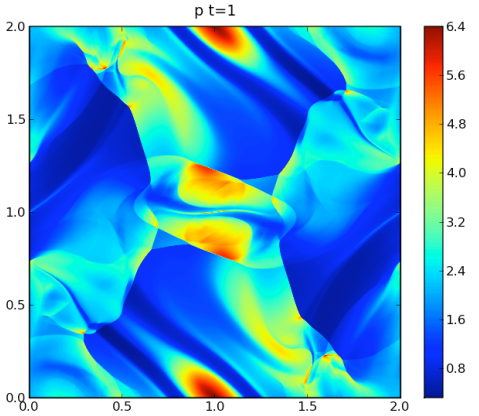

(d) 4000^2 mesh

FIGURE 1. Pressure for the Orszag-Tang vortex at time $t = 1$

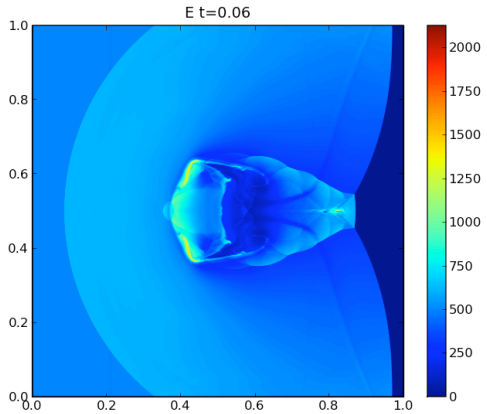

(a) Total energy

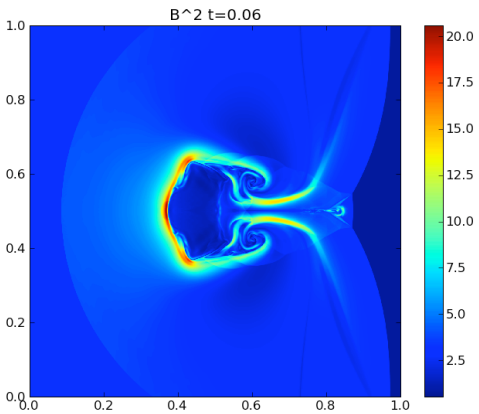

(b) Magnetic energy

FIGURE 2. Cloud-shock interaction at time $t = 0.06$ on a 1600^2 mesh.

Here, we assume that there exist a *potential* magnetic field $\widetilde{\mathbf{B}}$ satisfying the following assumptions,

$$\widetilde{\mathbf{B}}_t = 0, \quad \operatorname{div}(\widetilde{\mathbf{B}}) = 0, \text{ and } \operatorname{Curl}(\widetilde{\mathbf{B}}) = 0. \tag{3.2}$$

and solve for the perturbation $\mathbf{B} = \overline{\mathbf{B}} - \widetilde{\mathbf{B}}$.

Waves in the solar atmosphere are modeled as perturbations of the steady state:

$$\mathbf{u} \equiv \mathbf{0}, \quad \mathbf{B} \equiv 0 \quad \rho(z) = \frac{\rho_0 T_0}{T(z)} e^{-\frac{\alpha(z)}{H}}, \quad p(z) = p_0 e^{-\frac{\alpha(z)}{H}}. \tag{3.3}$$

Here,

$$\alpha(x,y,z) = \alpha(z) = \int_0^z \frac{1}{T(s)} ds, \tag{3.4}$$

with $T = T(z)$ being a given temperature distribution. An example for temperature distributions in the solar atmosphere is shown in figure 1. Here, ρ_0, p_0, H are constants.

Writing (3.1) in the condensed form, we obtain the balance law:

$$\mathbf{U}_t + f(\mathbf{U}, \widetilde{\mathbf{B}})_x + g(\mathbf{U}, \widetilde{\mathbf{B}})_y + h(\mathbf{U}, \widetilde{\mathbf{B}})_z = \sum_{l=1}^{3} \mathbf{s}^l(\mathbf{U}, \widetilde{\mathbf{B}}) + \mathbf{s}^g(\mathbf{U}), \tag{3.5}$$

The unknowns $\mathbf{U}$, fluxes f, g, h, co-efficient $\widetilde{\mathbf{B}}$, Godunov-Powell source $\mathbf{s}^{1,2,3}$ and gravity source $\mathbf{s}^g$ can be read from (3.1). A first-order finite volume scheme for (3.5) is given by,

$$\begin{aligned} \mathbf{W}_{i,j,k}^{n+1} = \mathbf{W}_{i,j,k}^n &- \Delta t^n \left(\frac{\mathbf{F}_{i+1/2,j,k}^n - \mathbf{F}_{i-1/2,j,k}^n}{\Delta x} + \frac{\mathbf{G}_{i,j+1/2,k}^n - \mathbf{G}_{i,j-1/2,k}^n}{\Delta y} \right) \\ &- \Delta t^n \left(\frac{\mathbf{H}_{i,j,k+1/2}^n - \mathbf{H}_{i,j,k-1/2}^n}{\Delta z} - \mathbf{S}_{i,j,k}^{1,n} - \mathbf{S}_{i,j,k}^{2,n} - \mathbf{S}_{i,j,k}^{3,n} - \mathbf{S}_{i,j,k}^{g,n} \right). \end{aligned} \tag{3.6}$$

The fluxes $\mathbf{F}, \mathbf{G}$ and sources $\mathbf{S}^{1,2}$ in the x- and y-directions are computed using the procedure outlined in section 2.

3.1. **Fluxes and sources in the z-direction.** The numerical flux $\mathbf{H}$ and discrete Godunov-Powell source term $\mathbf{S}^3$ in (3.6) are described in terms of the following Riemann problem,

$$\mathbf{W}_t + h(\mathbf{W}, \widetilde{\mathbf{B}}_m)_z = \mathbf{s}^3(\mathbf{W}, \widetilde{\mathbf{B}}_m, \mathbf{W}_z), \quad \mathbf{W}(z,0) = \begin{cases} \mathbf{W}_T & z < 0, \\ \mathbf{W}_B & z > 0. \end{cases}$$

The natural way to specify initial data $\mathbf{W}_{T,B}$ in the above problem is to use the states $\mathbf{W}_B = \mathbf{W}_{i,j,k}^n$ and $\mathbf{W}_T = \mathbf{W}_{i,j,k+1}^n$. However, this approach leads to a scheme that does not preserve discrete versions of the interesting steady states (3.3). Therefore we must design suitable fluxes in order to design well-balanced schemes.

3.1.1. *Local Hydrostatic pressure reconstructions.* Instead of just using the cell averages below and above the interface as data in the Riemann problem, we follow [5, 6] and utilize the special structure of the steady states (3.3) to perform a local hydrostatic reconstruction of the pressure inside the cell and use the local primitive variables,

$$\begin{aligned} \mathbf{V}_B &= \{\rho_{i.j,k}^n, \mathbf{u}_{i,j,k}^n, \mathbf{B}_{i,j,k}^n, p_{i,j,k+1/2}^{n,-}\} \\ \mathbf{V}_T &= \{\rho_{i,j,k+1}^n, \mathbf{u}_{i,j,k+1}^n, \mathbf{B}_{i,j,k+1}^n, p_{i,j+1/2}^{n,+}\}, \end{aligned}$$

where the reconstructed pressure is given in terms of extrapolated cell averages by first defining the local temperature,

$$T_{i,j,k}^n = \frac{p_{i,j,k}^n}{gH\rho_{i,j,k}^n}. \tag{3.7}$$

The piecewise constant temperature defines the scaling function α by (3.4). We can compute the differences in α and use it to define the reconstructed local pressure,

$$p^{n,-}_{i,j,k+1/2} = p^n_{i,j,k} e^{\frac{-\Delta z}{2HT^n_{i,j,k}}}, \quad p^{n,+}_{i,j,k+1/2} = p^n_{i,j,k+1} e^{\frac{\Delta z}{2HT^n_{i,j,k+1}}}, \tag{3.8}$$

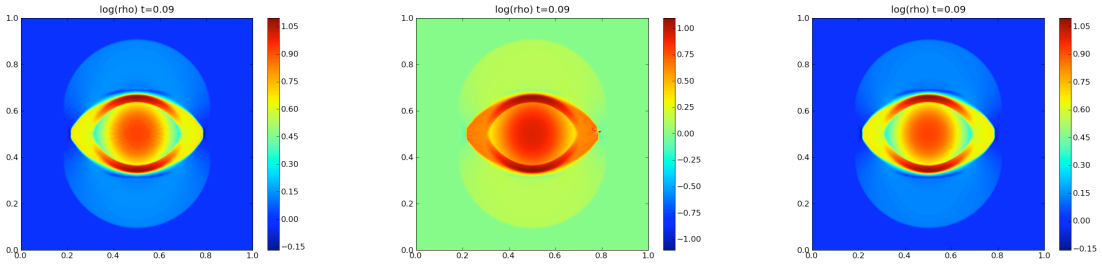

(a) No source (b) Central source (c) Upwind source

FIGURE 3. Density in the isothermal blast wave problem.

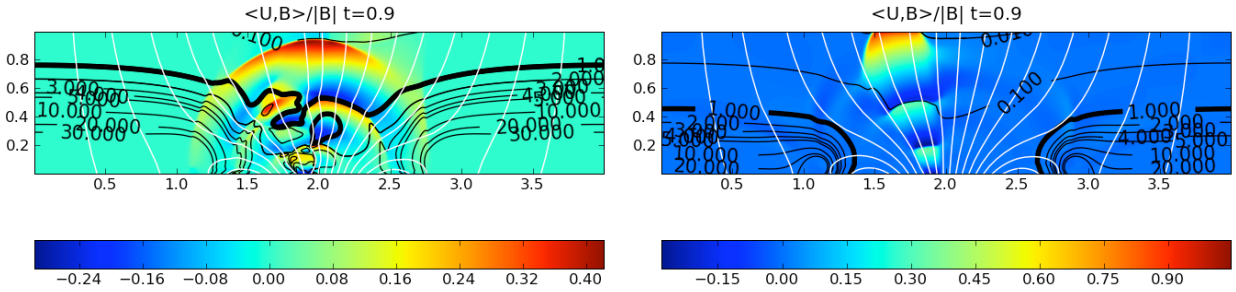

(a) Weak field (b) Strong field

FIGURE 4. Velocity in the direction of the magnetic field, computed with a second-order well-balanced scheme for the lower chromosphere.

The data $\mathbf{W}_B$ and $\mathbf{W}_T$ (in terms of conservative variables) are easily obtained from the primitive variables $\mathbf{V}_B$, $\mathbf{V}_T$. The coefficient $\widetilde{\mathbf{B}}_m$ is given by the average,

$$\widetilde{\mathbf{B}}_m = \widetilde{\mathbf{B}}_{i,j,k+1/2} = \frac{\widetilde{\mathbf{B}}_{i,j,k} + \widetilde{\mathbf{B}}_{i,j,k+1}}{2}. \tag{3.9}$$

The HLL three wave solver of the previous section is easily obtained for the z-direction by repeating the approach of describing the solver in the x- direction.

We discretize the gravitational source term as

$$\mathbf{S}^{g,n}_{i,j,k} = \left\{ 0, 0, \frac{p^{n,-}_{i,j,k+1/2} - p^{n,+}_{i,j,k-1/2}}{\Delta z}, 0, 0, 0, 0, -\rho^n_{i,j,k} (u^n_3)_{i,j,k}\ g \right\}. \tag{3.10}$$

where $p^{n,-}_{i,j,k+1/2}, p^{n,+}_{i,j,k-1/2}$ are defined in (3.8).

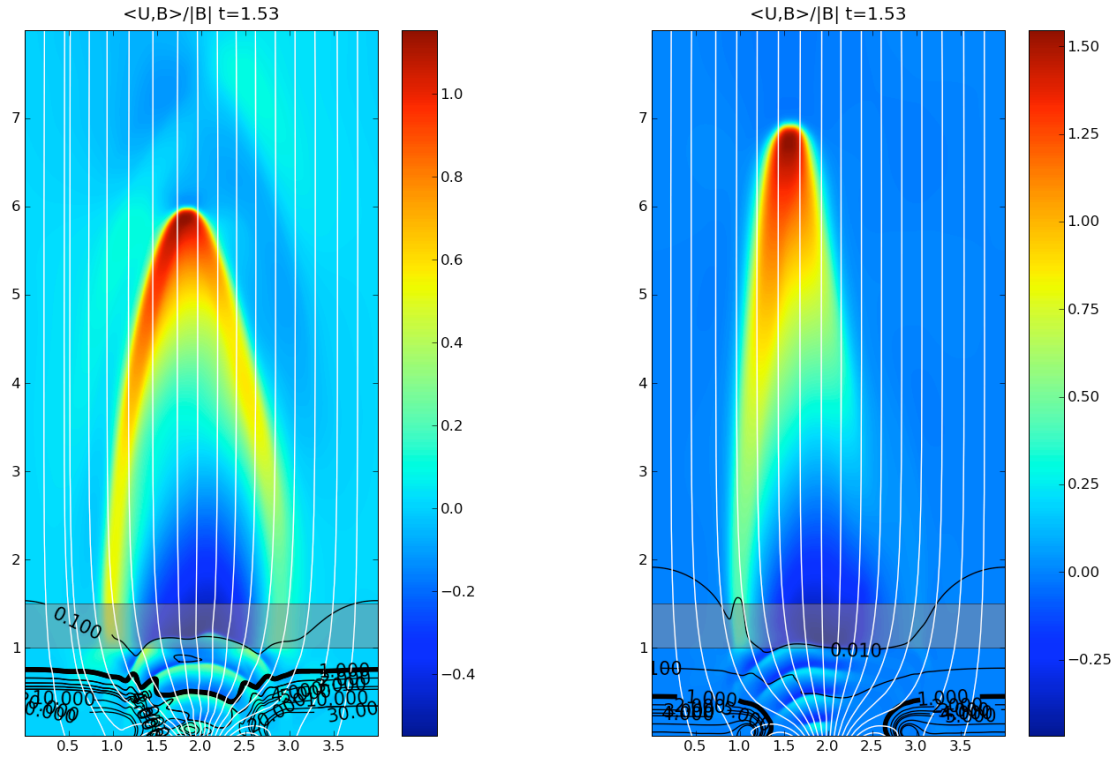

(a) Weak field (b) Strong field

FIGURE 5. Velocity in the direction of the magnetic field, computed with a second-order well-balanced scheme for both the chromosphere-corona.

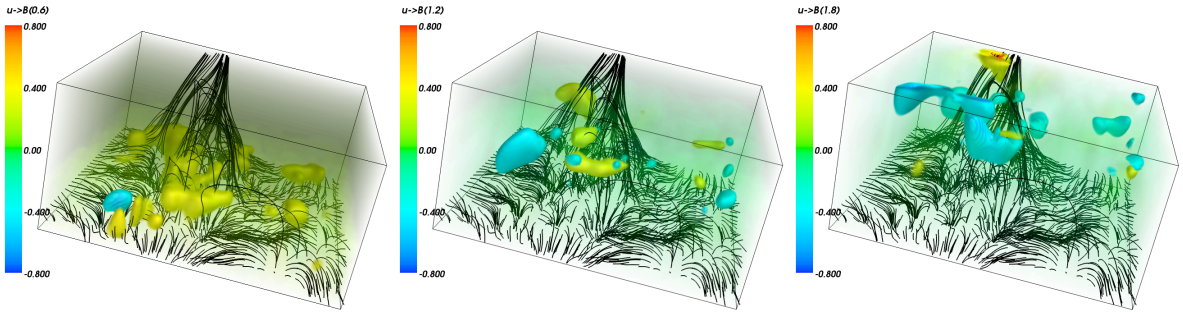

(a) t=0.6 (b) t=1.2 (c) t=1.8

FIGURE 6. Velocity in the direction of the magnetic field, computed with a second-order well-balanced scheme for the lower chromosphere with realistic magnetic field and velocity forcing.

Periodic boundary conditions are used in the x and y directions and we use the following *non-reflecting* Neumann type boundary conditions in the vertical direction:

$$\mathbf{W}^n_{i,j,0} = \mathbf{W}^n_{i,j,1} e^{\frac{\Delta z}{T_{i,j,1} H}}, \quad \mathbf{W}^n_{i,j,N_z+1} = \mathbf{W}^n_{i,j,N_z} e^{-\frac{\Delta z}{T_{i,j,N_z} H}}. \tag{3.11}$$

The resulting scheme satisfies the following properties.

Theorem 3.1. *Consider the scheme* (3.6) *approximating the system* (3.5). *This scheme has the following properties,*

(i.) *The scheme* (3.6) *is consistent with* (3.5)*, and it is first order accurate in both space and time (for smooth solutions).*

(ii.) *The scheme* (3.6) *is* well-balanced *and preserves discrete versions of the steady states* (3.3)*,*

The proof of the above theorem is presented in [6].

Remark 3.2. The finite volume scheme (3.6) is first-order accurate. For second-order accuracy, we need to employ locally hydrostatic piecewise linear non-oscillatory reconstructions as designed in [5, 6].

3.2. **Numerical experiments.**

3.2.1. *Waves in a two dimensional model solar atmosphere.* We consider a synthetic potential magnetic field $\widetilde{\mathbf{B}}$ given in [4] and plot the velocity (in the direction of the magnetic field) in two cases: first, with an isothermal atmosphere (modeling the lower chromosphere) and then with a realistic temperature distribution similar to the one shown in figure 1. Two magnetic field configurations are shown: one is a weak magnetic field and the other is a stronger magnetic field.

In figure 4, we plot the results for the lower chromosphere and in figure 5, we plot the results for the whole atmosphere, including the transition region and the corona. Both are computed with the second-order version of the well-balanced scheme (3.6). The results show the effectiveness of the schemes in resolving complex physical phenomena, in particular, the focusing of waves due to the magnetic field and the wave acceleration at the transition layer.

3.3. **Waves in a realistic solar chromosphere.**

Finally, we consider a background magnetic field measured from the MDI instrument on SOHO and bottom velocity measurements, also from SOHO and present the velocity (in the direction of magnetic field) in figure 6. The results demonstrate how the well-balanced schemes are robust and effective in simulating realistic scenarios in the solar atmosphere.

References

[1] T. J. Bogdan *et al.* Waves in the magnetized solar atmosphere II: Waves from localized sources in magnetic flux concentrations. *Astrophys. Jl,* 599, 2003, 626 - 660.

[2] J. U. Brackbill and D. C. Barnes. The effect of nonzero div$B$ on the numerical solution of the magnetohydrodynamic equations. *J. Comp. Phys.*, 35:426-430, 1980.

[3] F. Fuchs, S. Mishra and N. H. Risebro. Splitting based finite volume schemes for the ideal MHD equations. *J. Comp. Phys.,* 228 (3), 2009, 641-660.

[4] F. Fuchs, A. D. McMurry, S. Mishra, N. H. Risebro and K. Waagan. Approximate Riemann solver based high-order finite volume schemes for the Godunov-Powell form of ideal MHD equations in multi-dimensions. *Comm. Comput. Phys*, to appear
[5] F. Fuchs, A. D. McMurry, S. Mishra, N. H. Risebro and K. Waagan Well-balanced high-order finite volume methods for simulating wave propagation in stratified magneto-atmospheres. *J. Comput. Phys,* to appear.
[6] F. Fuchs, A. D. McMurry, S. Mishra, and K. Waagan Well-balanced high-order finite volume methods for simulating wave propagation in three-dimensional non-isothermal stratified magneto-atmospheres. *Preprint 2010.*, available from ftp://ftp.sam.math.ethz.ch/pub/sam-reports/reports/reports2010/2010-27.pdf
[7] *The ALSVID-SURYA home page,* http://folk.uio.no/ mcmurry/amhd.
[8] K. F. Gurski. An HLLC-type approximate Riemann solver for ideal Magneto-hydro dynamics. *SIAM. J. Sci. Comp.*, 25(6), 2004, 2165-2187.
[9] R. J. LeVeque. Finite volume methods for hyperbolic problems. *Cambridge university press,* Cambridge, 2002.
[10] K. G. Powell, P. L. Roe. T. J. Linde, T . I. Gombosi and D . L. De zeeuw, A solution adaptive upwind scheme for ideal MHD. J. Comp. Phys, 154(2), 284 - 309, 1999.
[11] G. Toth. The div$B$ $=$ 0 constraint in shock capturing magnetohydrodynamics codes. *J. Comp. Phys.*,161:605-652, 2000.

(S. Mishra) Seminar for Applied Mathematics (SAM),
D-Math, ETH Zürich,
HG G. 57.2, Rämistrasse, 101,
Zürich-8092, Switzerland.
E-mail address: smishra@sam.math.ethz.ch

Research Reports

No.	Authors/Title
10-37	*S. Mishra* Robust finite volume schemes for simulating waves in the solar atmosphere
10-36	*C. Effenberger, D. Kressner and C. Engström* Linearization techniques for band structure calculations in absorbing photonic crystals
10-35	*R. Hiptmair and C. Jerez-Hanckes* Multiple traces boundary integral formulation for Helmholtz transmission problems
10-34	*H. Harbrecht and Ch. Schwab* Sparse tensor finite elements for elliptic multiple scale problems
10-33	*K. Grella and C. Schwab* Sparse tensor spherical harmonics approximation in radiative transfer
10-32	*P. Kauf, M. Torrilhon and M. Junk* Scale-induced closure for approximations of kinetic equations
10-31	*M. Hansen* On tensor products of quasi-Banach spaces
10-30	*P. Corti* Stable numerical scheme for the magnetic induction equation with Hall effect
10-29	*H. Kumar* Finite volume methods for the two-fluid MHD equations
10-28	*S. Kurz and H. Heumann* Transmission conditions in pre-metric electrodynamics
10-27	*F.G. Fuchs, A.D. McMurry, S. Mishra and K. Waagan* Well-balanced high resolution finite volume schemes for the simulation of wave propagation in three-dimensional non-isothermal stratified magneto-atmospheres
10-26	*U.S. Fjordholm, S. Mishra and E. Tadmor* Well-balanced, energy stable schemes for the shallow water equations with varying topography
10-25	*U.S. Fjordholm and S. Mishra* Accurate numerical discretizations of non-conservative hyperbolic systems